Astron. Astrophys. 344, 282–288 (1999)

ASTRONOMY AND ASTROPHYSICS

Computing radiative equilibria with Monte Carlo techniques

L.B. Lucy⋆

Space Telescope – European Coordinating Facility, Karl-Schwarzschild-Strasse 2, D-85748 Garching bei München, Germany

Received 7 September 1998 / Accepted 9 December 1998

Abstract. Monte Carlo techniques are used iteratively to compute the radiative equilibrium temperature stratification of a non-grey, spherically-extended stellar atmosphere in LTE. The derived temperature distribution agrees well with that predicted by Castor's (1974) code, as also does the emergent spectrum. However, in contrast to such conventional codes, the adopted Monte Carlo techniques and associated temperature-correction procedure are in no way restricted to 1-D stratifications. Accordingly, this successful test indicates that realistic 2- and 3-D radiative equilibria can be similarly computed.

Key words: radiative transfer – methods: numerical – stars: atmospheres

1. Introduction

The theoretical investigation of many astrophysical phenomena requires the accurate determinations of ambient and emergent radiation fields. Nowadays, with the ready availability of powerful computers, this is usually accomplished by solving the equation of radiative transfer numerically. Thus, derivatives and integrals are approximated by differences and summations, and the resulting algebraic system solved by matrix inversion, with an outer iteration loop being required when the absorption and scattering coefficients are coupled to the radiation field due to their dependence on state variables. For problems with a high degree of symmetry, such as plane-parallel stellar atmospheres or spherically-symmetric stellar winds, this conventional numerical approach can hardly be faulted and has indeed led to powerful codes that accurately solve these 1-D problems, even with full non-LTE treatments of excitation and ionization of numerous elements. However, as astronomers' interests turn increasingly to 2- and 3-D problems, this approach becomes problematical, for the number of variables to be solved for then becomes huge, as do the codes themselves. Moreover, most of the iterative schemes fundamental to the success of these existing codes are specific to 1-D geometry.

When geometrical simplicity is lost, the Monte Carlo approach to transfer problems becomes attractive and may often be the only feasible technique. Indeed, inspection of the astrophysical literature reveals numerous cases where the Monte Carlo method has been applied specifically to treat complexities that would defeat or severely test the conventional approach. Some recent examples are: studying the penetration of UV radiation into the interiors of clumpy interstellar clouds (Boissé 1990), treating resonance-line scattering in accretion disk winds (Knigge et al. 1995), and computing polarization maps for the circumstellar envelopes of protostars (Fischer et al. 1994). It is noteworthy, however, that in these examples and indeed in most Monte Carlo transfer codes the absorption and scattering coefficients are not coupled to the radiation field. Evidently, such problems, which require solution by iteration, have for the most part been avoided by developers of Monte Carlo codes.

When a problem is solved iteratively, corrections are applied at each iteration, and these are derived from the residuals that express the previous solution's failure to satisfy the problem's basic equations. An obvious concern, therefore, when contemplating Monte Carlo techniques, is that these residuals will at some stage be dominated by sampling errors, thus possibly halting the convergence of the iterative sequence before a solution of the desired accuracy has been achieved. In fact, this is exactly the problem that thwarted Price (1969) in his ambitious attempt to calculate a non-LTE, plane-parallel, radiative equilibrium stellar atmosphere with Monte Carlo methods. At large optical depths, the flux residuals were dominated by sampling errors and so the temperature corrections were meaningless.

Nevertheless, with today's computer power and with appropriate Monte Carlo techniques, problems requiring solution by iteration are feasible. A recent example is the work of Och et al. (1998), who iteratively determined the temperature and ionization stratification for a photoionized nebula of uniform density using a Monte Carlo treatment of radiative transfer, obtaining good agreement with the predictions of conventional codes both for the nebula's structure and its emission line spectrum. Since their Monte Carlo code is not fundamentally restricted to spherical symmetry, it can readily be generalized to treat realistic 3-D models of inhomogeneous nebulae.

In this paper, another such 1-D test problem is treated, namely that of computing the temperature stratification and emergent spectrum of an extended spherical non-grey stellar atmosphere in LTE, a problem solved with conventional methods by Castor (1974). The particular investigation described here was initially carried out in 1988 with the aim of including

Send offprint requests to: L.B. Lucy

⋆ *Present address:* Astrophysics Group, Blackett Laboratory, Imperial College of Science, Technology and Medicine, Prince Consort Road, London SW7 2BZ, UK

continuum formation in a Monte Carlo code (Abbott & Lucy 1985) developed to investigate the dynamical consequences of multi-line transfer effects in hot star winds and was briefly alluded to by Schmutz et al. (1990). Although successful, this work was in the end omitted from the code developed for Wolf-Rayet winds (Lucy & Abbott 1993 – see Sect. 2.3) in order to avoid two nested iteration loops. Nevertheless, the omitted technique is likely to be useful in other astrophysical contexts, as indicated by similar, but not identical work briefly described by Bjorkman & Wood (1997). As with the work of Och et al. (1998), the techniques described herein readily generalize to 2 and 3-D problems.

2. Test problems

In order to test Monte Carlo codes, it is necessary to apply them first to special cases where simplifying assumptions have allowed exact or highly accurate solutions to be derived with conventional analytic or numerical techniques. Here, where the aim is to derive the temperature distribution throughout a medium in radiative equilibrium, the simplest test cases are provided by the theory of grey stellar atmospheres. In this case, the exact solution is known for plane-parallel geometry (the Hopf function) and accurate numerical solutions are available for spherical, extended atmospheres.

Although results for grey atmospheres will be briefly reported, they are essentially trivial in the present context, in that they do not test our ability to improve solutions iteratively in the presence of Monte Carlo noise. Accordingly, a more meaningful and challenging test problem has been sought from the extensive literature on *non*-grey stellar atmospheres computed under the assumption of local thermodynamic equilibrium (LTE).

The chosen problem is that considered by Castor (1974). Motivated by evidence that the continuum-forming layers in the Of star ζ Puppis and in a number of Wolf-Rayet stars are extended, he created *static* model atmospheres having this characteristic by considering stars of exceptionally high luminosity-to-mass ratios. Using a method based on moment equations and requiring iteration on Eddington factors and on ratios of mean absorption coefficients, Castor computed both the structure of these extended atmospheres and their emergent spectra.

In view of its closely similar scientific motivation, Castor's work provided a natural test problem for testing Monte Carlo techniques that would allow the Abbott-Lucy code to include continuum formation in model winds for hot stars. However, because of this aim, an acceptable technique should not merely reproduce Castor's results, it must also permit the treatment of line transfer – fundamental to the dynamics of the winds – and allow radiative equilibrium to be imposed in the matter frame rather than the rest frame (Lucy & Abbott 1993). The technique described below meets these conditions as well as not being restricted to 1-D geometry.

In Castor's work, both the density and the temperature stratification were computed. However, given our present understanding of the *dynamical* causes of atmospheric extension in hot stars, solving for the complete structure of a static atmosphere that is extended because of high L/M now seems little more than an academic exercise. Accordingly, we focus here just on the problem of deriving the temperature distribution from the condition of radiative equilibrium. Thus, the principal test problem is the following: given the density stratification $\rho(r)$ predicted by Castor's code, derive the corresponding temperature stratification $T(r)$ as well as the resulting emergent luminosity density L_ν.

3. Monte Carlo procedures

In this section, the Monte Carlo methods used to obtain the temperature distribution in an extended, spherically symmetric, non-grey stellar atmosphere are described. These methods represent a continuation and extension of previous work on stellar winds (Abbott & Lucy 1985; Lucy & Abbott 1993), supernovae (Lucy 1987; Mazzali & Lucy 1993), and photoionized nebulae (Och et al. 1998).

3.1. Energy packets and radiative equilibrium

In Monte Carlo treatments of radiative transfer, we can take the calculation's "quanta" to be photons, thereby simulating exactly the physical processes occurring as matter and radiation interact. However, we also have the freedom to take the quanta to be packets of photons of the same frequency so that $\varepsilon(\nu) = nh\nu$ is the energy content of a packet containing n photons. This is often advantageous. For example, taking all packets to have the same energy $\varepsilon(\nu) = \varepsilon_0$ implies that packets in the infrared have large numbers of photons that one thereby avoids following individually (Abbott & Lucy 1985).

In this investigation, photons are also grouped into packets of constant energy but now with the motivation of rigorously imposing the constraint of zero flux divergence on the Monte Carlo radiation fields derived for an iterative sequence of approximate temperature distributions. Thus, when a packet of radiant energy $\varepsilon(\nu_a) = \varepsilon_0$ suffers a pure absorption event, it is re-emitted with frequency ν_e in accordance with the emissivity of the medium and with energy

$$\varepsilon(\nu_e) = \varepsilon(\nu_a)\ . \tag{1}$$

This simple but powerful device constrains the radiation field to be divergence-free at each and every iteration, and this has the following consequence: For a not-yet-converged temperature stratification, this Monte Carlo radiation field will in general be a closer approximation to the final radiative equilibrium solution than would be that derived by actually solving the equation of radiative transfer. Accordingly, successively bringing matter into thermal equilibrium with a sequence of such divergence-free radiation fields should result in rapid convergence, with acceptable results if sampling errors are small enough.

As the above remarks imply, with the adopted procedure, the derived Monte Carlo radiation fields only represent solutions of the equation of radiative transfer when the temperature distribution has converged to the radiative equilibrium solution, for only

then does Eq. (1), which implies a balance between the rates of absorption and emission of energy, correspond to physical reality. Apart from sampling errors, the divergence-free radiation fields at early iterations differ from the final solution only in consequence of the temperature dependence of the absorption and scattering coefficients. Accordingly, for grey atmospheres "convergence" is immediate, since successive temperature iterates then differ only because of different sampling errors.

3.2. Initiation

In order to carry out the Monte Carlo calculation, the extended atmosphere is approximated by J spherical shells, with the jth shell having inner and outer radii R_j and R_{j+1}, and these radii are such that R_{j+1}/R_j is constant. Within each shell, the density ρ, the temperature T, and the scattering and absorption coefficients σ, k_ν are constant. This crude, low-accuracy discretization is common practice in Monte Carlo treatments of radiative transfer because it simplifies the sampling of flight paths. The shell densities ρ_j are obtained from Castor's code; the other variables are derived iteratively as the radiative equilibrium solution is found.

At the lower boundary $r = R_1$, the outwardly-directed radiation field is taken to be

$$I_\nu^+ = B_\nu(T_b) \tag{2}$$

– i.e. isotropic in the outward hemisphere with black body intensity at unknown "boundary" temperature T_b. Using the current estimate of T_b, energy packets are selected according to this boundary condition as follows:

(1) The mid-probability points ν_k of K equal probability bins for black body emission are determined from the equation

$$\frac{k-\frac{1}{2}}{K} = \int_0^{\nu_k} B_\nu d\nu \;/\; \int_0^\infty B_\nu d\nu \tag{3}$$

with k = 1, 2, …, K. Note that this calculation can be done in terms of the frequency variable $h\nu/kT_b$, and so need not be repeated when T_b changes.

(2) An integer k is chosen randomly from the interval $(1, K)$ and the frequency of the emitted packet set = ν_k.

(3) The initial direction cosine is taken to be

$$\mu = \sqrt{z}\;, \tag{4}$$

where here and below z denotes a random number from the interval $(0, 1)$.

In practice, it is beneficial to depart from step (2) by introducing stratified sampling for the frequency distribution of packets emitted at the lower boundary. Thus, in fact, we constrain Poisson noise by selecting equal numbers of packets from each of the K frequency bins.

The frequency sampling at the lower boundary can be checked by computing the mean value of $h\nu/kT_b$. For black body emission, this should = 3.83223.

3.3. Trajectories

Having thus launched a packet across the lower boundary, we must now compute its trajectory as it scatters off free electrons and undergoes absorptions followed by re-emissions due to bound-free and free-free processes. This trajectory ends when the packet escapes to infinity or re-enters the core by crossing the lower boundary. Notice that because of Eq. (1), packets do not disappear within the atmosphere. Nor, in this scheme, are packets spontaneously created within the atmosphere.

Within each uniform shell, the random flight path of a packet between events is

$$\tau_\nu = -\ln(z)\;, \tag{5}$$

which corresponds to the physical displacement ℓ given by

$$\tau_\nu = (k_\nu + \sigma)\rho\ell\;. \tag{6}$$

If this displacement would carry the packet out of its current shell, then the packet is moved along its linear flight path to the boundary with the next shell, at which point a new τ_ν is selected and its further progress followed in the next shell. On the other hand, if this displacement leaves the packet within the current shell, then at the end-point of the displacement the packet is either scattered or undergoes absorption followed by re-emission. We take this physical event to be a scattering if

$$z < \frac{\sigma}{k_\nu + \sigma} \tag{7}$$

and to be an absorption otherwise.

Note that the selection of a new τ_ν when a packet crosses a boundary does not result in bias: a photon always has τ_ν = 1 as the expected path length to its next interaction no matter what distance it has already travelled.

After a physical event, the packet's frequency and direction cosine must be re-assigned. If the event was a scattering, the frequency is unchanged – i.e., assumption of coherent electron scattering. If the event was an absorption, the re-emitted packet is assigned frequency ν given by the equation

$$z = \int_0^\nu j_\nu d\nu \;/\; \int_0^\infty j_\nu d\nu\;, \tag{8}$$

where $j_\nu = k_\nu B_\nu$ is the emissivity. In either case, the new direction cosine is selected according to the rule

$$\mu = -1 + 2z\;, \tag{9}$$

corresponding to isotropic scattering or emission.

As with frequency sampling at the lower boundary, the operation indicated by Eq. (8) is in practice replaced by a pre-iteration calculation of equal probability emissivity bins, and so it is the label of the bin that is randomly selected in assigning a frequency to a re-emitted packet. Note that these bins change from shell to shell and must be recomputed after each temperature-correction step.

When these emissivity bins are calculated, the mean frequency of the emissivity function for each shell can also be calculated. These can then be used to check the mean frequencies of the packets re-emitted during the Monte Carlo calculation.

3.4. Monte Carlo estimators

In order to detect departures from radiative equilibrium, we must first calculate the rate at which matter absorbs energy from the radiation field, and this must be derived from the Monte Carlo model of the radiation field. Now, the exact expression for this quantity is

$$\dot{A} = 4\pi \int_0^\infty k_\nu J_\nu d\nu \; , \tag{10}$$

and in radiative equilibrium this balances the rate at which matter emits energy, given by

$$\dot{E} = 4\pi \int_0^\infty k_\nu B_\nu d\nu \; . \tag{11}$$

Evidently, to compute $\dot{A}$, we must first compute the mean intensity J_ν. Now, in constructing Monte Carlo estimators for moments of the radiation field, the natural starting point is the basic definition of specific intensity in terms of energy flow in a given direction across a reference surface. This is the approach adopted by Och et al. (1998), leading to an estimator for J_ν given in their Eq. (13). However, for problems without symmetries, there will in general be no unique or natural reference surfaces for the volume elements of the adopted discretization. Accordingly, with respect to J_ν and weighted integrals thereof, it is preferable to construct Monte Carlo estimators from the basic result that the energy density of the radiation field in $(\nu, \nu + d\nu)$ is $4\pi J_\nu d\nu \,/\, c$.

At a given instant, a packet contributes energy $\varepsilon(\nu) = \varepsilon_0$ to the volume element containing it. Accordingly, if ℓ denotes the path length between successive events, where "events" includes crossings of boundaries between volume elements, then this segment of a packet's trajectory contributes $\varepsilon_0 \delta t \,/\, \Delta t$ to the time-averaged energy content of a volume element, where $\delta t = \ell / c$ and Δt is the duration of our Monte Carlo experiment. The estimator for the volume element's energy density that follows from this argument gives the following estimator for the monochromatic mean intensity

$$J_\nu d\nu = \frac{1}{4\pi} \, \frac{\varepsilon_0}{\Delta t} \, \frac{1}{V} \sum_{d\nu} \ell \; , \tag{12}$$

where V is the volume and the summation is over all flight segments in V for packets with frequencies in $(\nu, \nu + d\nu)$. The corresponding estimator for the integrated mean intensity is

$$J = \frac{1}{4\pi} \, \frac{\varepsilon_0}{\Delta t} \, \frac{1}{V} \sum \ell \tag{13}$$

where the summation is now over all segments in V regardless of frequency.

If we now compare Eqs. (6) and (12), we see immediately that a Monte Carlo estimator for the absorption rate is

$$\dot{A} = \frac{\varepsilon_0}{\Delta t} \, \frac{1}{V} \sum k_\nu \ell \; . \tag{14}$$

This is the expression used below in an iterative scheme to find the radiative equilibrium ($\dot{A} = \dot{E}$) solution.

It is worth noting that these estimators are such that all packets entering the volume element V contribute. With estimators based on a reference surface within V, some packets will enter and depart from V without crossing that surface and so do not contribute. This, together with the total freedom allowed in the shapes of the volume elements, strongly suggest the superiority of this approach.

A further point to emphasize is that packets contribute to our estimate of the absorption rate even if they pass through V without being absorbed. Indeed, Eq. (14) returns estimates of the absorption rates throughout a model atmosphere even when that atmosphere is so tenuous that all packets pass through without absorption. This is a point of difference with the investigation of Bjorkman & Wood (1997), where the absorption rate is computed only from the packets that are absorbed in the volume element. If the estimator is thus restricted to absorbed packets, the result is noisier, is indeterminate in the optically thin limit, and we have failed to use our knowledge of the exact formula given in Eq. (10).

3.5. Temperature corrections

If N packets are launched across the lower boundary in our Monte Carlo experiment and N_∞ of these ultimately escape to infinity, then our estimate of the star's luminosity is

$$L(\infty) = N_\infty \frac{\varepsilon_0}{\Delta t} \; . \tag{15}$$

Since the factor $\varepsilon_0 / \Delta t$ has hitherto remained free, we now fix it by setting $L(\infty) = L_*$, the desired luminosity of the model.

With $\varepsilon_0 / \Delta t$ thus determined, Eq. (14) now gives the absorption rate throughout the atmosphere in physical units, and in general this rate will not balance the emission rate given by Eq. (11) – i.e. $\dot{A}(r) \neq \dot{E}(r)$. To obtain a modified temperature distribution that brings the atmosphere closer to radiative equilibrium, we note that $\dot{E}$ can be written as

$$\dot{E} = 4\pi k_{\rm P} B \; , \tag{16}$$

where $k_{\rm P}$ is the Planck-mean absorption coefficient and $B = (\sigma/\pi) T^4$ is the integral of the Planck function. This then suggests that the temperature distribution for the next iteration should be that given by

$$B = \frac{\dot{A}}{4\pi k_{\rm P}} \; , \tag{17}$$

with quantities on the right-hand side evaluated from the just-completed iteration. This is the adopted temperature-correction procedure, with only the slight modification that an undercorrection factor ~ 0.5–0.8 is commonly used.

Readers familiar with temperature-correction procedures for non-grey atmospheres will recognize that Eq. (17) can be written as

$$B = \frac{k_J}{k_{\rm P}} \, J \; , \tag{18}$$

where k_J is the intensity- or absorption-mean absorption coefficient. Thus, the adopted scheme is *apparently* identical to the

notorious lambda-iteration procedure that has long been known to fail (see, e.g., Mihalas 1970). However, this failure relates to its use with conventional transfer techniques and can be traced to the fact that Eq. (18) gives a "correction" without using information about the required constant value of $L(r)$. Here the Monte Carlo radiation field itself carries this information and, in fact, at all iterations rigorously obeys the constraint $L(r) = L_*$. Thus the adopted procedure can be described as bringing the matter into equilibrium with a radiation field that already has the correct $L(r)$, and the procedure only fails to converge immediately because k_ν depends on T.

The boundary temperature T_b, which determines the frequency distribution but not the luminosity L^+ of the radiation emitted at the lower boundary, must also be iteratively improved. Now, integration of Eq. (2) gives

$$L^+ = 4\pi R_1^2 \times \sigma T_b^4 \, , \tag{19}$$

and we also have

$$L^+ = N \frac{\varepsilon_0}{\Delta t} \, . \tag{20}$$

Accordingly, after completion of a Monte Carlo step, $\varepsilon_0/\Delta t$ is obtained as noted earlier from Eq. (15). Eq. (20) then gives L^+, which on substitution in Eq. (19) yields an improved value for T_b. The implied correction is, however, applied with the same undercorrection factor used above when iteratively correcting $T(r)$.

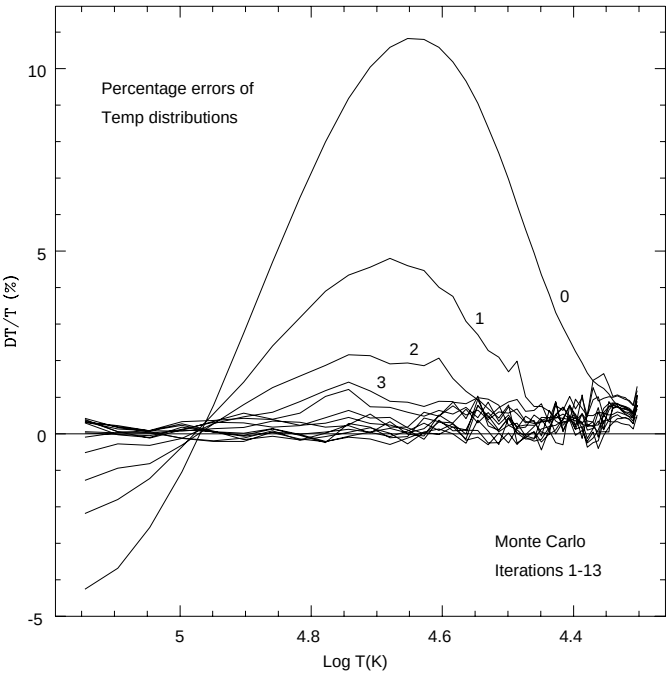

Fig. 1. Percentage errors of the iteratively-derived temperature distributions plotted against the exact temperature of each spherical shell as given by Castor's (1974) code. The initial model (0) as well as the first three iterates are labelled.

4. Numerical results

In this section, the Monte Carlo technique and the temperature-correction procedure described in Sect. 3 are used to derive the radiative equilibrium solution for the density stratification given by Castor's (1974) code.

4.1. Parameters

The basic parameters for the extended, spherical atmosphere are $L_* = 9.37 \times 10^5 L_\odot$, $M = 30 M_\odot$, and a composition of pure hydrogen. With these parameters, $\Gamma_e = \sigma L/4\pi GMc = 0.95$. The luminosity is therefore close to the Eddington limit, and so the atmosphere is distended by the greatly reduced effective gravity.

As Castor (1974) himself pointed out, such high values of Γ_e are not achieved by stars in their hydrogen-burning phases, and so this mechanism is certainly not relevant for the extended continuum-forming layers of Of stars. The interest here is that the resulting stratification makes sphericity important. Moreover, the Schuster mechanism in such extended, scattering-dominated atmospheres results in the Lyman continuum being in emission. Together, these aspects of Castor's (1974) work provide a challenging test for the Monte Carlo approach.

For the Monte Carlo calculation, the lower boundary is taken to be at $R_1 = 9.089\, R_\odot$, corresponding to Rosseland mean optical depth $\tau_R = 7.13$ according to Castor's code. The constant ratio R_{j+1}/R_j is set = 1.053 as in Castor's calculation, a choice that eliminates the need for interpolation when comparing temperature distributions. With these choices, the number of shells is $J = 43$, and the outer radius is $R_{J+1} = 84.236\, R_\odot$.

In sampling black body emission at the lower boundary and the emissivity in each shell, $K = 1000$ equal probability bins are used.

4.2. Temperature corrections

With the above parameters, Castor's code computes $\rho(r)$, $T(r)$ and the emergent spectrum. For the Monte Carlo calculation, this $\rho(r)$ is taken as given and an initial guess $T_0(r)$ made for the temperature distribution. With two state variables thus known, the degree of ionization of hydrogen and the scattering and absorption coefficients can be calculated for all shells. Together with an initial guess T_b^0 for the boundary temperature, these coefficients then allow a Monte Carlo step to be made. At the completion of this step, a divergence-free model of the ambient radiation field is available, from which an improved temperature distribution $T_1(r)$ and an improved boundary temperature T_b^1 are computed as described in Sect. 3.5. This procedure is then repeated until "convergence" is achieved.

In Fig. 1, the results of 13 such iterations are shown in a Monte Carlo experiment for which $N = 500\,000$ is the number of packets emitted at the lower boundary. Since Castor's code provides an essentially exact $T(r)$, the plotted quantity is $(T_i - T)/T_i$ rather than $(T_i - T_{i-1})/T_{i-1}$, the fractional change from the previous approximation.

From Fig. 1, we see that the iterations (with an overly cautious undercorrection factor = 0.5) converge rapidly until $i \simeq 5$ but thereafter exhibit apparently random fluctuations about a mean that agrees to better than 1% with Castor's solution. For most astrophysical purposes, both the amplitude of the fluctuations after "convergence" and the accuracy of recovering a known solution are entirely satisfactory. (A slight anomaly at the surface may be seen in Fig. 1, in the form of a slight uptick in the fractional errors of all iterates. This is due to the way the ρ_j were derived from Castor's model, which results in his surface value being assigned to the *mid-point* of the outermost shell in the Monte Carlo calculation.)

Although of little consequence, the displacement from Castor's solution is systematic and therefore merits investigation. When the calculation is repeated with the lower boundary higher in the atmosphere – i.e., larger R_1 – this systematic displacement increases. This suggests that the problem is the approximation – Eq. (2) – used as the lower boundary condition, and which is valid only in the limit $\tau_R \to \infty$. Nevertheless, there may also be a contribution to the displacement from small differences in the two codes' treatments of the absorption coefficient as well as from the cruder discretizations used in the Monte Carlo calculation.

4.3. Grey atmospheres

As a further check on systematic error, the Monte Carlo code has been applied to the essentially trivial problem of computing grey atmospheres in radiative equilibrium.

In the plane-parallel case, the lower boundary is placed at $\tau_1 = 2$, and the limb-darkening law obeyed by the emitted packets is linear with coefficient $u = 3/(5 + 3\tau_1)$, which would be exact if $T(\tau)$ for $\tau > \tau_1$ were the Milne-Eddington solution. In an experiment with $N = 5 \times 10^6$ packets, the derived temperature distribution matched that calculated with the Hopf function with root mean square error = 0.021% and maximum error = 0.045%. These are negligibly small compared to the offset in Fig. 1 from Castor's solution.

In this same Monte Carlo experiment, the mean intensity is also calculated as in Och et al. (1998) using reference surfaces at the mid-points of the slabs into which the plane-parallel atmosphere is discretized. The resulting temperature distribution obtained by setting $B = J$ has root mean square error = 0.031% and maximum error = 0.061%. These are moderately inferior to the results above and therefore support the preference for volume-based mean intensity estimators.

The Monte Carlo code has also been applied to spherical grey atmospheres, specifically to the calculations of Hummer & Rybicki (1971). In an experiment with $N = 500\,000$, their temperature distribution for opacity index $n = 3/2$ and outer radius $r = 100$ is reproduced with root mean square error = 0.061% and maximum error = 0.20%.

These grey atmosphere successes confirm that high precision can be achieved with this Monte Carlo code and that the slight offset in the non-grey test case is not a consequence of the adopted technique.

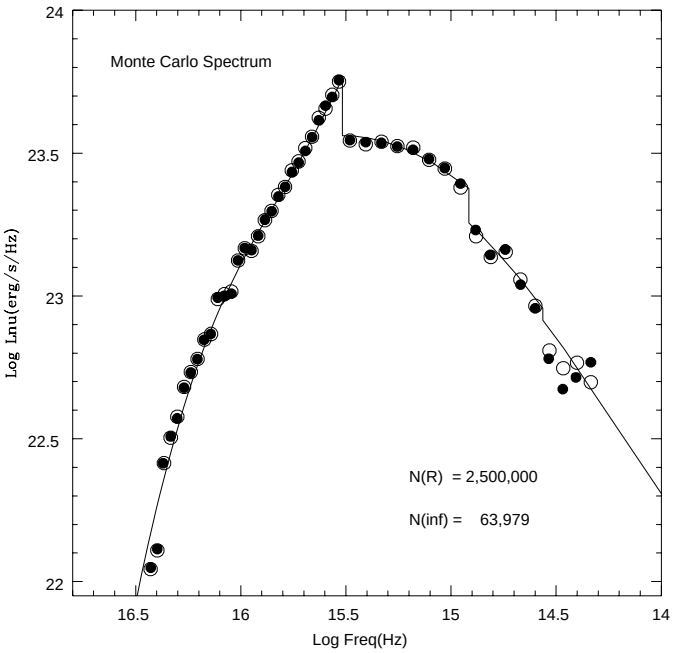

Fig. 2. The Monte Carlo spectrum (filled circles) derived from 63,979 escaping packets compared to the spectrum predicted by Castor's (1974) code (solid line). Also plotted (open circles) is the spectrum obtained from the formal integral using the source function derived from the Monte Carlo model of the ambient radiation field.

4.4. Emergent spectrum

Having demonstrated in Sect. 4.2 that the iterative scheme reproduces Castor's temperature distribution with acceptable accuracy, we now compare emergent spectra. With the temperature distribution from the 13th iteration – an unnecessarily large number of iterations, in fact – a further Monte Carlo step is carried out with N increased by a factor of 5 to 2.5×10^6 packets. Of these, $N_\infty = 63\,979$ escape to infinity and their distribution in frequency constitutes the Monte Carlo prediction for the emergent spectrum. This prediction (filled circles) is shown in Fig. 2, together with the spectrum predicted by Castor's conventional transfer calculation.

Comparison of the two theoretical spectra reveals excellent agreement in the Lyman and Balmer continua. In particular, the operation of the Schuster mechanism in inverting the Lyman discontinuity has evidently been accurately modelled. A significant fall-off in accuracy is, however, seen in the IR and EUV. This is of course a consequence of the small number of escaping packets in these frequency bins and illustrates the limited dynamical range of Monte Carlo calculations.

In 2- or 3-D problems, it will often be desirable to compute spectra as seen from different orientations after deriving the temperature stratification with a technique such as described here. This can be done via the formal integral for the emergent intensity – i.e., by computing the intensity observed along multiple lines-of-sight to the object when viewed at the required orientation and then summing to obtain the luminosity density L_ν. But to do this, the mean intensity J_ν is needed in order to evaluate the source function at points along these lines-of-sight.

In fact, the necessary estimator is given by Eq. (12), which converts to physical units when $\varepsilon_0/\Delta t$ is determined by forcing the Monte Carlo calculation to be consistent with the luminosity of the source(s) illuminating the domain of calculation.

A formal-integral calculation of the emergent spectrum using the source function thus extracted from the $N = 2.5 \times 10^6$ simulation has been carried out with the familiar $p - z$ cylindrical coordinates. The resulting spectrum is plotted in Fig. 2 as open circles and is seen to agree closely with the spectrum derived from escaping packets.

5. Conclusions

The aim of this paper has been to develop and test Monte Carlo techniques for deriving radiative equilibrium temperature distributions when the absorption and scattering coefficients depend on state variables and are thus coupled to the ambient radiation field. In solving a non-trivial test problem, we have demonstrated that the iterative approach effectively required for such problems is not precluded by Monte Carlo noise. Indeed, by constructing Monte Carlo radiation fields that are rigorously divergence-free, rapid convergence is achieved with a temperature-correction procedure that is formally identical to the notoriously unsuccessful Λ-iteration method. This resurrection of the Λ-iteration method is in fact of considerable importance since the resulting temperature-correction procedure – see Eq. (17) – is geometry-independent. Thus, unlike most standard temperature-correction schemes, which are constructed to achieve constant flux or constant luminosity variable, the procedure presented here immediately generalizes to 2- and 3-D problems. Moreover, this generalization is facilitated by the volume-based intensity estimators derived in Sect. 3.4.

In conclusion, the successful reproduction of Castor's solution for an extended, non-grey atmosphere implies that realistic 2- and 3-D problems that similarly require solution by iteration can be tackled with some confidence using Monte Carlo techniques. Moreover, in sharp contrast with conventional methods, the Monte Carlo codes will remain modest in size and can therefore be quickly constructed and verified.

Acknowledgements. The non-grey model atmosphere used to test the Monte Carlo code was calculated by D.C. Abbott with Castor's code at JILA in 1988. He also provided unpublished information about the ionization and absorption coefficient routines in that code.

References

Abbott D.C., Lucy L.B., 1985, ApJ 288, 679
Bjorkman J.E., Wood K., 1997, BAAS 29, 1227
Boissé P., 1990, A&A 228, 483
Castor J.I., 1974, ApJ 189, 273
Fischer O., Henning Th., Yorke H.W., 1994, A&A 284, 187
Hummer D.G., Rybicki G.B., 1971, MNRAS 152, 1
Knigge C., Woods J.A., Drew J.E., 1995, MNRAS 273, 225
Lucy L.B., 1987, In: Danziger I.J. (ed.) Proceedings of the ESO Workshop on SN 1987A, p. 417
Lucy L.B., Abbott D.C., 1993, ApJ 405, 738
Mazzali P., Lucy L.B., 1993, A&A 279, 447
Mihalas D., 1970, Stellar Atmospheres. W.H. Freeman & Co., San Francisco, p. 170
Och S.R., Lucy L.B., Rosa M.R., 1998, A&A 336, 301
Price M.J., 1969, Ap&SS 4, 182
Schmutz W., Abbott D.C., Russel R.S., Hamann W.-R., Wessolowski U., 1990, ApJ 355, 255